Impurity-seeding experiments on JET in preparation for the ITER-like wall

G Maddison[1], K McCormick[2], C Giroud[1], A Alonso[3], B Alper[1], Y Andrew[1], G Arnoux[1], P Belo[4], M Beurskens[1], A Boboc[1], S Brezinsek[5], M Brix[1], I Coffey[6], E de la Luna[3], P de Vries[1], S Devaux[2], T Eich[2], R Felton[1], W Fundamenski[1], D Harting[5], J Hobirk[2], A Huber[5], S Jachmich[7], I Jenkins[1], E Joffrin[8], A Kallenbach[2], M Kempenaars[1], M Lehnen[5], T Loarer[8], P Lomas[1], D McDonald[1], A Meigs[1], P Morgan[1], J Ongena[7], V Riccardo[1], F Rimini[9], A Sirinelli[1], M Stamp[1], G Telesca[7], H Thomsen[2], and JET EFDA contributors[*]

JET-EFDA, Culham Science Centre, Abingdon, OX14 3DB, UK.

[1] EURATOM/UKAEA Fusion Association, Culham, Abingdon, Oxon. OX14 3DB, UK.
[2] Max-Planck IPP, EURATOM Association, D-85748 Garching, Germany.
[3] Asociación EURATOM-CIEMAT, Laboratorio Nacional de Fusion, Spain.
[4] CFN, EURATOM-IST Associação, 1096 Lisbon, Portugal.
[5] FZ Jülich GmbH, Institut für Plasmaphysik, Association EURATOM-FZJ, Jülich, Germany.
[6] Queen's University Belfast, University Road, Belfast BT7 1NN, Northern Ireland, UK.
[7] Association 'Euratom-Belgian state', Ecole Royale Militaire, B-1000 Brussels, Belgium.
[8] Association EURATOM-CEA, CEA Cadarache, F-13108 St Paul lez Durance, France.
[9] EFDA-JET CSU, Culham Science Centre, Abingdon, Oxon. OX14 3DB, UK.
[*] *see appendix of F Romanelli et al, Fusion Energy (Proceedings 22nd International Conference, Geneva, 2008) IAEA.*

1. Introduction

A major advance towards development of ITER operating regimes will be made on JET by installation of an all metal, ITER-like wall (ILW), consisting of a beryllium first-wall and tungsten divertor. The latter in particular will feature W-coated CFC side and base tiles, with a solid W main plate, composed of 4 toroidal rings or "stacks", to receive the outboard strike-point. These new materials imply revised, stringent constraints on tolerable loadings, which eg for the solid W target set surface temperature limits (initially ≈ 1200°C to avoid recrystallisation, later ≈ 2200°C) and / or energy limits (≈ 50 MJ per stack, for a wetted fraction of ≈ 0.7) [1]. Simultaneously exclusion of carbon, primarily to lower fuel retention, is expected to reduce its presently large contribution to radiated power. Addressing both issues in principal ITER-relevant scenarios being studied on JET naturally suggests trials of raised recycling and seeding with extrinsic impurities, although this latter involves an additional limit on near-target temperatures (less than ~ 10 eV) to avoid excessive sputtering of tungsten. Results are reported from a series of systematic fuelling and seeding scans, Fig.1, in high-triangularity

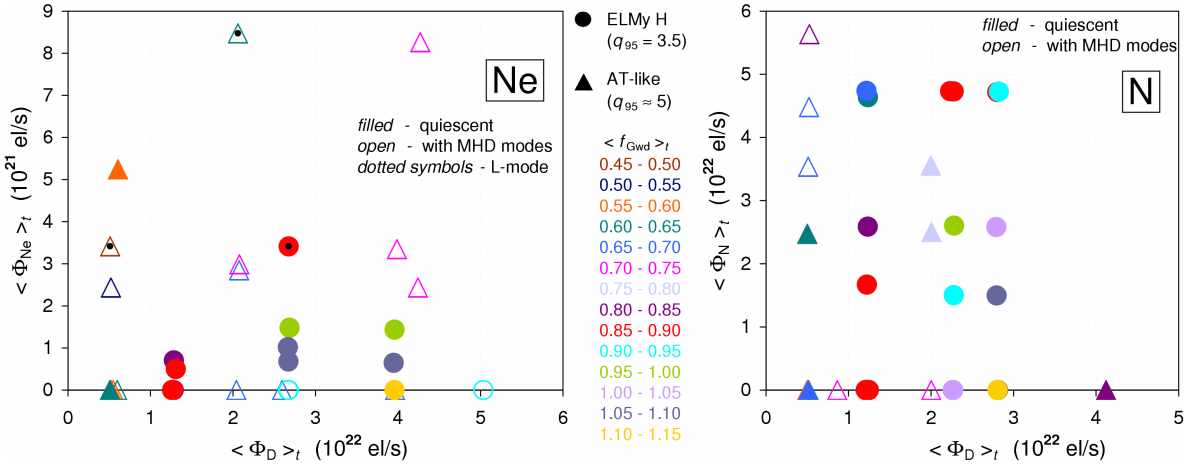

Fig.1 Fuelling / seeding scans conducted, in terms of input rates of D and Ne (left) or N (right) as electrons $\cdot s^{-1}$ assuming full ionisation, averaged over the flat-top phase of each pulse. Note the very different vertical scales. (Points colour-coded for the Greenwald density fraction averaged over a 1 - 2 s interval.)

ELMy H-mode (EH, 2.7 T, 2.5 MA, $q_{95} \approx 3.5$, $\delta^{av} \approx 0.41$, $P_{NB+RF} \approx 15$ MW) and advanced-tokamak-like (AT, 2.7 T, 1.8 MA, $q_{95} \approx 5.0$, $\delta^{av} \approx 0.39$, $P_{NB+RF} \approx 22$ MW) plasmas, which were intended to characterise their operational domains from standard to detached behaviour. Attention is focused particularly on moderation of underlying loads between ELMs, as a possible adjunct to separate active ELM mitigation techniques. Both neon and nitrogen impurities were examined, to exploit their contrasting recycling, ionisation and radiation properties. For AT-like cases, these experiments extend the range of earlier studies [2]. Preliminary analyses of the coupling between pedestal properties and recycling in the outboard divertor are given in a companion paper [3].

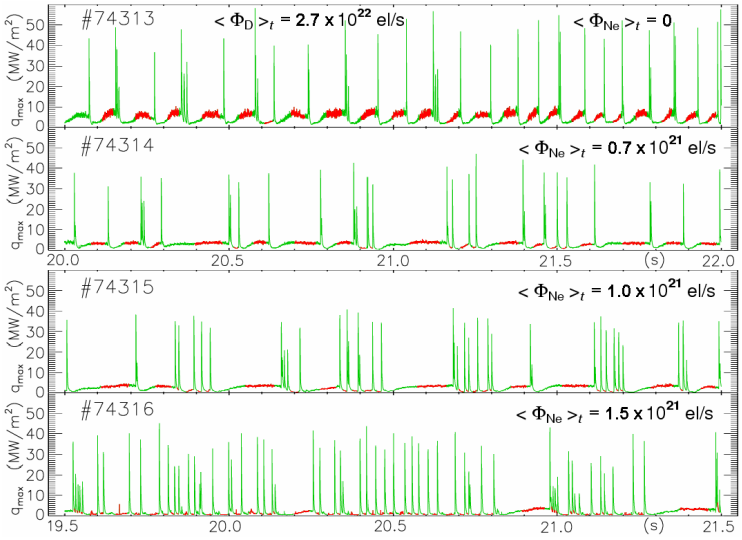

Fig.2 Variation of ELMs during Ne scan at medium D fuelling, illustrating selected inter-ELM periods highlighted in red.

2. Radiation fraction and target loading

Seeding with either impurity species tends to induce more compound ELMs, so that frequencies become difficult to define categorically. Generally they are increased in both EH (between ≈ 10 to ≈ 100 Hz) and AT-like (between ≈ 100 to ≈ 1000 Hz) cases. Divertor target loadings are detected with a new fast infra-red camera, which frames at a sufficient rate (typically ≈ 12 kHz here) to be able to resolve inter-ELM periods throughout. To infer associated plasma properties, signals are projected onto time intervals chosen to be from 50% to 90% of the way between successive ELM peaks, the half-way point being intended to avoid most of each post-ELM-crash recovery. They are then averaged within a flat-top window typically 1 - 2 s long (see Fig.2). Other, more slowly sampled quantities such as Greenwald density fraction f_{Gwd} and energy confinement normalised to ITER98(y,2) scaling H_{98y} are

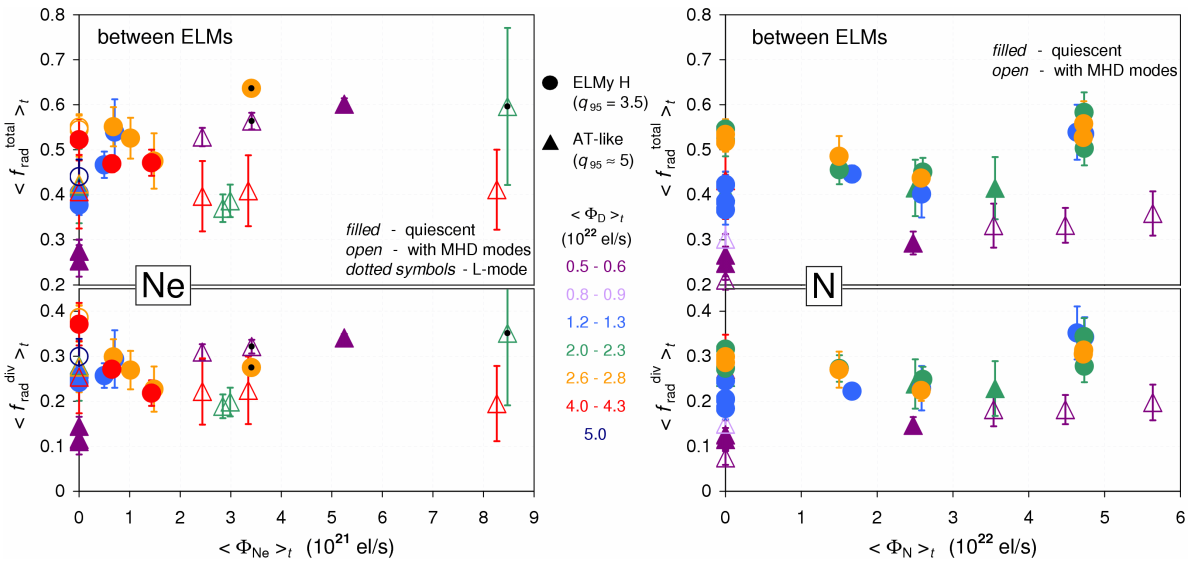

Fig.3 Total (top) and divertor (bottom) radiated power fractions averaged between ELMs during the flat-top of each pulse seeded with Ne (left) or N (right). Note the very different horizontal scales.

averaged over the whole window. Uncertainties are estimated in all instances from the square root of the variance in each time averaging. Note nitrogen exhibits a clear legacy effect from shot to shot in the present carbon machine (see Fig.4) which can hinder the more sensitive break-down of AT scenario and inhibited the breadth of its fuelling – seeding scan (Fig.1).

From the $< f_{\mathrm{Gwd}} >_t$ coding in Fig.1 it can be seen that stronger D fuelling leads to higher density for ELMy H-modes, but adding either Ne or N generally causes their density to fall again, particularly at higher D input. Density is less affected by either fuelling or seeding in AT-like plasmas, although by design these are at lower normalised (and absolute) levels. Similarly $< H_{98y} >_t$ is degraded in either scenario (see Fig.5) by rising D_2 puffing and appears further decreased by seeding with Ne. However, AT-like plasmas especially were prone to (3,2) and sometimes (2,1) neo-classical tearing modes (indicated in figures) which were apt to degrade their confinement, obscuring any such impact of seeding itself. Highest Ne inputs tend to revert to L-mode regime. Within the scans, line-average $< Z_{\mathrm{eff}} >_t$ is also increased by up to 100% with Ne and still deteriorates by up to ≈ 70% with N. The key effect upon radiated power fraction between ELMs is depicted in Fig.3. This base level of emission is first increased by stronger D_2 puffing alone, commensurate with a strong rise in outboard divertor recycling [3]. Except at lower D fuelling, seeding then adds only a modest further increment in $< f_{\mathrm{rad}}^{\text{i-E}} >_t$, and can actually cause some loss of radiation in ELMy H-modes, probably owing to the fall in density. In all cases, total radiation fraction remains below ≈ 65%, recalling this apparent empirical limit found before on JET [4]. The ratio of divertor to bulk emission, discriminated by those portions respectively under and above the X-point, changes little with either impurity rate or species, and is actually highest (≈ 1.5 to ≈ 2.5) for strong D input without seeding. Note the very high values of N injection, in terms of electrons $\cdot\, \mathrm{s}^{-1}$, which can be tolerated to achieve the same range of $< f_{\mathrm{rad}}^{\text{i-E}} >_t$. Eventually this would reach the radiative Type III regime demonstrated previously on JET [4].

Accompanying moderation of divertor loads is illustrated in Fig.4 by average peak power density between ELMs incident on the outboard target. Again it falls markedly for mounting recycling produced by stronger D fuelling, then can be lowered further by adding either Ne or N, down to levels ≈ 1 MW $\cdot\, \mathrm{m}^{-2}$ approaching detachment. This amelioration of exhaust onto the plate receiving the outboard strike-point (see inset in Fig.4) for relatively little or even a negative change in radiation suggests there may also be some spatial redistribution of efflux power by impurities, at least in ELMy H-modes. Tentative support is lent by a smaller proportional change in total divertor energies detected by embedded thermocouples.

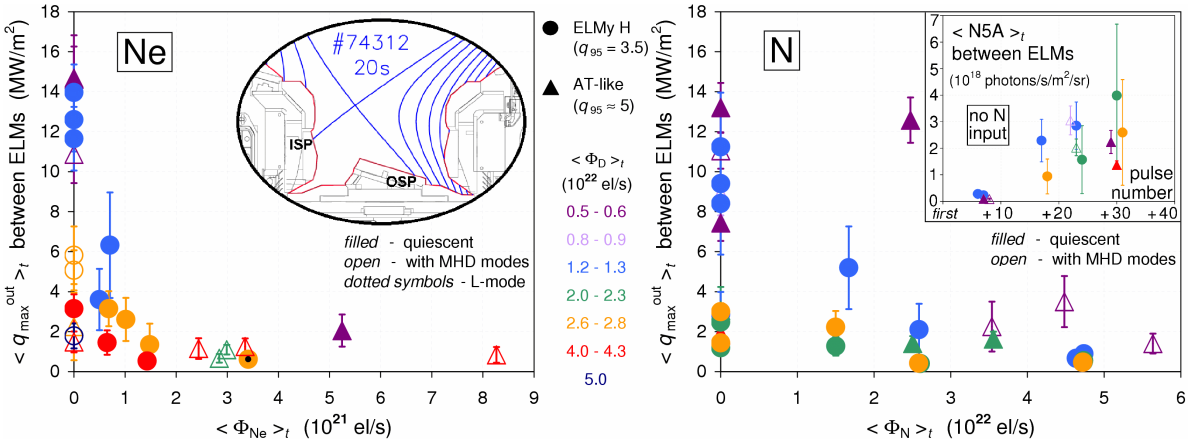

Fig.4 Peak power density on the outboard divertor target measured by fast thermography, averaged between ELMs during the flat-tops of cases with Ne (left) or N (right). Inset (left): EFIT reconstruction of the divertor configuration. Inset (right): illustration of the shot to shot N legacy effect, by divertor intensity between ELMs of N V line at 20.93 nm in shots with no N input, interspersed throughout the scans.

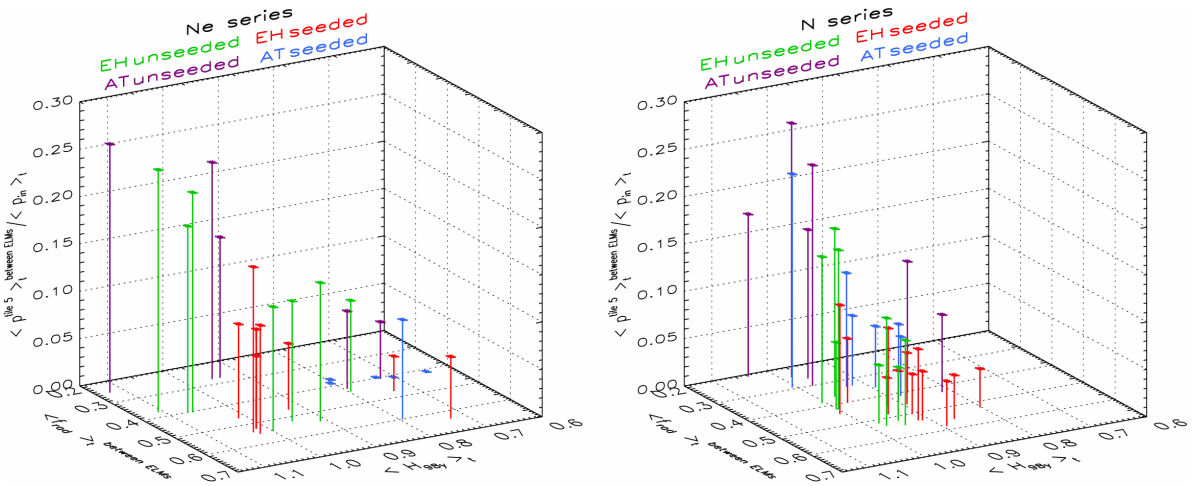

Fig.5 Power landing on the outboard divertor target between ELMs, normalised to total input power, versus normalised energy confinement and radiation fraction between ELMs. All averages during flat-top phases. Left: Ne series (points shown as zero are undetermined within measurement uncertainties). Right: N series.

3. Discussion

Behaviour observed in both scenarios with D fuelling and Ne or N seeding is summarised in Fig.5. Average power between ELMs received by the full outboard target plate (divertor tile 5), normalised by total input power, is shown as a function of average normalised confinement and radiation fraction between ELMs. Ideal performance in this projection would be represented by access into the front bottom left corner of the diagram. It can be seen that standard loadings in ELMy H-modes and AT-like plasmas can be significantly reduced by raised recycling effected by stronger D_2 puffing (green, violet points), although at the expense of some loss of confinement. Here H_{98y} is estimated from the thermal energy confinement time calculated from plasma profiles measured by high-resolution Thomson scattering recently implemented on JET. Some further small improvement in loads can be induced by adding Ne or N (red, blue points), while incurring only a minor extra decrement in confinement. Lower atomic number N seems to be milder than Ne in this respect, mostly retaining at least $< H_{98y} >_t \approx 0.9$ throughout (though remembering the caveat implied by different levels of MHD activity), and also regarding incremental $< Z_{eff} >_t$. Radiation fraction cannot be increased beyond ≈ 60% in any case without reverting to L-mode. Final target powers achieved between ELMs would appear to be compatible with the new limits of the ILW, but it should be borne in mind that average values including ELMs are less affected by seeding (within much larger variances), tending to be largest in higher power AT-like pulses. In other words, ELMs can retain a persistent capacity to exhaust power, as well as inducing severe transients not significantly buffered by radiation [5]. This re-emphasizes the importance of combining elevated recycling and impurity seeding with methods for active ELM control.

4. References

1. V Riccardo *et al* 12th International Workshop on Plasma-Facing Materials and Components for Fusion Applications , Jülich, Germany, May 2009
2. M Beurskens *et al* Nuclear Fusion **48** (2008) 095004
3. K McCormick *et al* P2-161 *this conference*
4. J Rapp *et al* Nuclear Fusion **44** (2004) 312
5. P Monier-Garbet *et al* Nuclear Fusion **45** (2005) 1404

Work conducted under EFDA and partly supported by the UK Engineering & Physical Sciences Research Council and the European Community under the contract of Association between EURATOM and UKAEA. The views and opinions expressed herein do not necessarily reflect those of the European Commission.